

GaAsSb-BASED HBTs GROWN BY PRODUCTION MBE SYSTEM

H. J. Zhu, J. M. Kuo, P. Pinsukanjana, X. J. Jin, K. Vargason,
M. Herrera, D. Ontiveros, C. Boehme, and Y. C. Kao

Intelligent Epitaxy Technology, Inc., 1250 E. Collins Blvd., Richardson, TX 75081, USA

Abstract

This work investigates the growth of GaAsSb base DHBTs with InP and InAlAs emitters using a multi-wafer production MBE system. Favorable hole mobilities were measured for carbon-doped GaAsSb from $4.3E19\text{cm}^{-3}$ to $1.8E20\text{cm}^{-3}$ compared to their counterparts grown by MOCVD and gas-source MBE. Highly uniform GaAsSb epilayer with Sb composition fluctuation of less than $\pm 0.1\%$ across a 4" wafer was obtained in our multi-wafer MBE system. Large area devices of GaAsSb DHBTs fabricated with InAlAs emitters have better device characteristics than their InP emitter counterparts. The feasibility of multi-wafer MBE for mass production of GaAsSb-based HBTs was demonstrated through the extremely high uniformity of 4" GaAsSb wafer and the excellent electrical properties of InAlAs/GaAsSb/InP DHBTs.

I. Introduction

InP-based heterojunction bipolar transistors (HBTs) have emerged as the technology of choice for 40 Gb/s communication systems. Recently, InGaAs-base InP SHBTs with record high $f_t > 500\text{GHz}$ [1] and static flip-flop circuits based on InP/InGaAs/InP DHBT technology with toggle speed of 151 GHz [2] have been demonstrated. Although InGaAs-based DHBTs with InP collectors provide higher breakdown voltages and much better thermal conductivity than InGaAs collectors used in SHBTs, the InGaAs/InP base-collector junction conduction band discontinuity is a source of current blocking. To eliminate this current blocking problem, complicated composition grading between the base and the collector are necessary. On the other hand, the current blocking problem can be alleviated by replacing the conventional InGaAs base with $\text{GaAs}_{0.51}\text{Sb}_{0.49}$ material. The type II band alignment between InP and $\text{GaAs}_{0.51}\text{Sb}_{0.49}$ permits the implementation of uniform InP as the collector with an abrupt collector-base heterojunction, while maintaining the advantages of InP collector [3-5]. In fact, DHBTs with GaAsSb base have recently attracted much attention, and MOCVD-grown InP/GaAsSb/InP abrupt DHBTs have been demonstrated with both f_T and f_{MAX} as high as 300 GHz at high operating current density [6].

By far, InP has been the most chosen emitter material for InP/GaAsSb DHBTs. However, the negative conduction band discontinuity of the InP emitter with respect to the GaAsSb base is an inherent disadvantage for InP/GaAsSb emitter-base junction. Current blocking may be a problem at the emitter-base junction, especially in the high current density operation conditions. Moreover, it is not trivial to grow a quality InP emitter on GaAsSb base using MBE. Therefore, it is important to explore different emitter

materials, which have proper conduction band alignment with respect to GaAsSb. In addition, since GaAsSb is a mixed group V compound semiconductor, composition uniformity is a very challenging issue for small single wafer MBE system, let alone large multi-wafer system. To our knowledge, there is no report on the growth of InP/GaAsSb DHBTs by multi-wafer MBE in the literature.

In this paper, we demonstrate that highly uniform GaAsSb with state-of-the-art hole mobility can be obtained on 4" wafer in our multi-wafer MBE machine. We also report that GaAsSb HBTs with InAlAs emitter have better device characteristics than their counterparts with InP emitter. The importance of in-situ sensors, such as absorption band edge spectroscopy (ABES) [7, 8] and optical-based flux monitor (OFM) [9, 10] for monitoring and control of the growth conditions during the production environments is also illustrated.

II. Experimental

A Riber 49 multi-wafer MBE system equipped with standard effusion cells for group III elements was used for this study. Separate crackers for As and P, as well as a solid-source Sb cracker were used to investigate the growth of GaAsSb and GaAsSb-based DHBTs. Si was used for the n-type doping, while CBr_4 from a low-temperature gas injector was used for p-type doping. The growth temperature was measured by ABES measurements and the group III fluxes were monitored by OFM. The optimal growth conditions were obtained by systematically varying the substrate temperature, the total group V pressure, and the As/Sb flux ratio.

Test wafers of 100 nm thick carbon-doped GaAsSb were grown on (100) InP:Fe substrates using the optimal growth

conditions. Following the epitaxial growth, the samples underwent structural, and electrical characterization. Double crystal x-ray diffraction in the (400) orientation was used to measure the GaAsSb composition. Hall measurements were carried out using the standard van der Pauw method.

III. Results and Discussion

A. Hole Mobility

Featureless surfaces with excellent morphology were found in all the grown samples. The x-ray diffraction peak of the $\text{GaAs}_{1-x}\text{Sb}_x$ was typically within 200 arc-sec of the InP substrate peak. This was corresponding to less than 1% mismatch ($x=0.487\pm 0.01$) to InP substrates. Figure 1 shows the room temperature hole mobility of the carbon-doped GaAsSb as a function of the hole concentration. Hole concentration up to $1.8 \times 10^{20} \text{ cm}^{-3}$ were achieved with the MBE grown GaAsSb. The hole mobility decreases from $46 \text{ cm}^2/\text{V}\cdot\text{sec}$ to $27 \text{ cm}^2/\text{V}\cdot\text{sec}$ as the hole concentration increases from $4.3 \times 10^{19} \text{ cm}^{-3}$ to $1.8 \times 10^{20} \text{ cm}^{-3}$. The hole mobilities exhibit a weak dependence on doping level, which is consistent with the reports of carbon-doped GaAsSb in the literature. Strong alloy scattering in GaAsSb accounts for the relative low hole mobilities compared to carbon-doped InGaAs [11,12]. Favorable hole mobility values were obtained by our MBE as compared to the counterparts of carbon-doped GaAsSb by MOCVD [12, 13] and GSMBE [13].

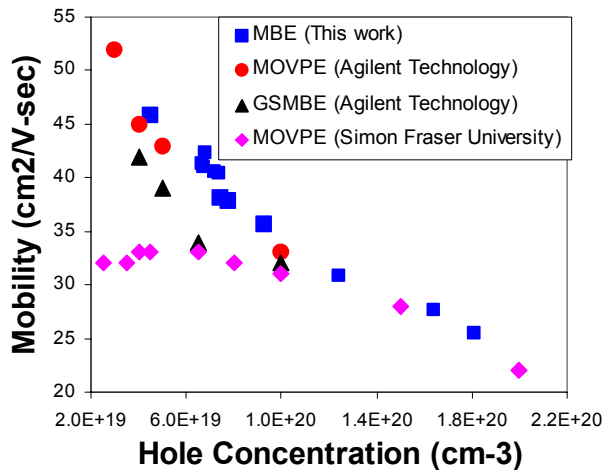


Fig. 1: Room temperature hole mobility of CBr_4 -doped GaAsSb as a function of carrier concentration.

B. Uniformity

Currently, most InGaAs/InP HBT circuits in the industry are fabricated with processing lines of 4" InP wafers. The first important steps for the development of GaAsSb DHBT technology are improvement of composition uniformity as well as the uniformity of carbon concentration in 4" InP wafers. Any non-uniformity in the composition and doping concentration of the GaAsSb:C

will affect the base-emitter voltage of the HBT and, hence, the performance of the HBT circuits. In order to develop multi-wafer GaAsSb DHBTs for industrial use, a growth of 100 nm CBr_4 doped GaAsSb on a 4" InP:Fe wafer using 4 x 4" platen were performed. The growth was purposely mismatched so that the diffraction peak of GaAsSb could be easily distinguished from the InP:Fe substrate peak. Fig. 2 shows the rocking curves of the carbon-doped 4" GaAsSb wafer measured at multiple points along the diameter of the wafer in the radiant direction of the platen. The GaAsSb diffraction peaks are ~ 500 arc-sec away from the InP substrate peak position. Their shapes and peak positions are almost identical to each other for all the measured positions. This indicates that the substrate temperature distribution is very uniform along the radiant direction of the 4 x 4" platen, since the compositions of mixed group V epilayers are very sensitive to the substrate temperature. X-ray rocking curves of the 4" GaAsSb eplayer at different locations on the same radius were also checked to verify the azimuthal composition uniformity. Fig. 3 summarizes the composition

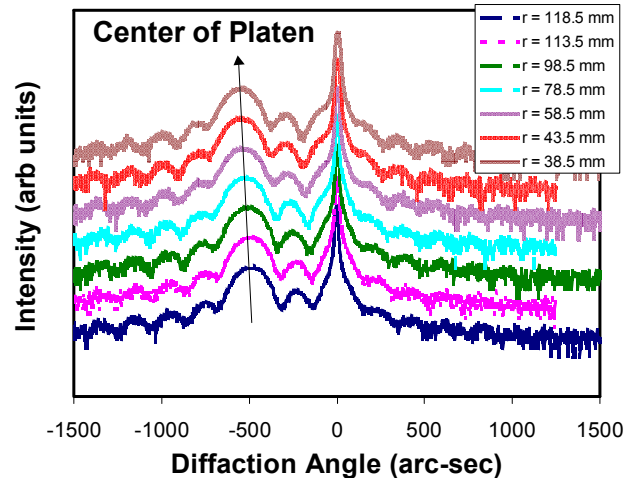


Fig. 2: Double-crystal x-ray diffraction spectra of a 4" GaAsSb at different locations along the radiant direction on the 4 X 4" platen.

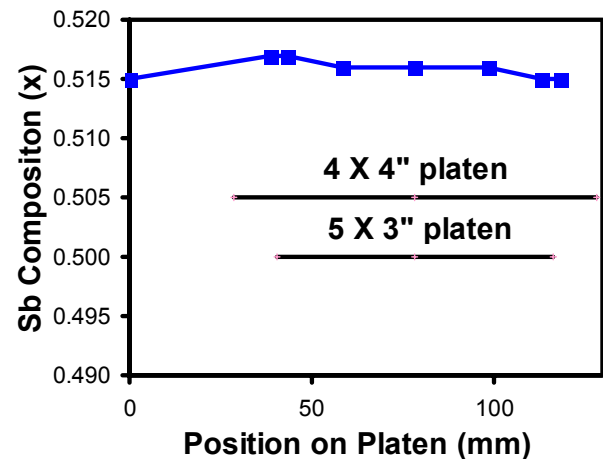


Fig. 3: Uniformity of $\text{GaAs}_{1-x}\text{Sb}_x$ composition across the platens of a Riber 49 MBE system.

uniformity variation of the 4" GaAsSb:C grown on this 4 x 4" platen. The Sb composition fluctuation is less than $\pm 0.1\%$ across the 4" wafer and the whole platen. This is attributed to the success of our modification on the Sb cracker and the optimal growth conditions of GaAsSb.

The uniformity of carbon doping concentration across the 4" GaAsSb epilayer was revealed by the Leighton resistivity map, which was measured by a 36-point scan with 5 mm exclusion zone. The average sheet resistance was ~ 347.1 Ohm/square, with a cross-wafer standard deviation of $\sim 2.3\%$. This uniformity of sheet resistivity is adequate for GaAsSb based DHBT process development. The uniformity of carbon doping concentration can be further improved with design optimization of the CBr4 injector showerhead.

C. InAlAs/GaAsSb/InP DHBTs

To further evaluate the material quality of the GaAsSb:C grown with the production MBE reactor, the growth of GaAsSb/InP DHBTs with InP and InAlAs emitter, was explored. Figure 4 shows an example of the ABES taken during a complete InAlAs/GaAsSb/InP DHBT growth. It was possible to reproduce the HBT characteristics from run to run by repeating the ABES growth temperature profile in GaAsSb based HBTs. ABES data was critical because infrared pyrometry was not effective in the substrate temperature range used.

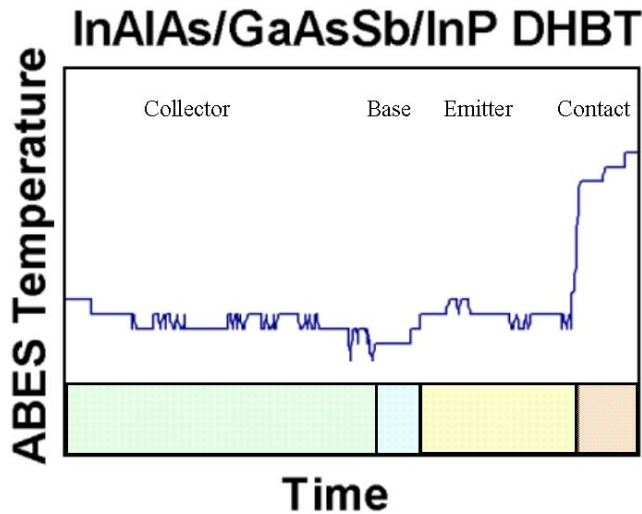


Fig. 4: ABES substrate temperature profile of an InAlAs/GaAsSb/InP DHBT during the growth in Riber 49.

Large-area devices (LADs) of GaAsSb DHBTs with InP and InAlAs emitters were fabricated. The emitter mesa size was $50\ \mu\text{m} \times 50\ \mu\text{m}$. Fig. 5 shows the common emitter I_c - V_{ce} characteristics of an InAlAs/GaAsSb/InP DHBT with 40 nm base thickness and $4.5E19\ \text{cm}^{-3}$ base doping. The InP:Si collector thickness is 200 nm. The LAD has $BV_{cco} > 6V$ with dc current gain of 45 at $1\text{kA}/\text{cm}^2$. The base sheet resistivity is ~ 1000 Ohm/sq as measured by the transmission line method (TLM). In contrast, the dc

current gain is only 13.5 at $1\text{kA}/\text{cm}^2$ for the GaAsSb HBT with InP emitter, which has otherwise the same structure and growth conditions. This can be attributed to the strong atomic interaction of Ga and P atoms at the InP/GaAsSb interface. Fig. 6 shows the Gummel plot of an InAlAs/GaAsSb/InP DHBT with $1E20\ \text{cm}^{-3}$ carbon doping and 20 nm in base thickness. The crossover for collector and base current is at 5 nA. The dc current gain is 22 at $1\text{kA}/\text{cm}^2$. The collector and base ideality factor is 1.08 and 1.30, respectively. The base sheet resistance is ~ 956 Ohm/sq. These device characteristics clearly demonstrate that our InAlAs/GaAsSb/InP DHBTs are of high quality.

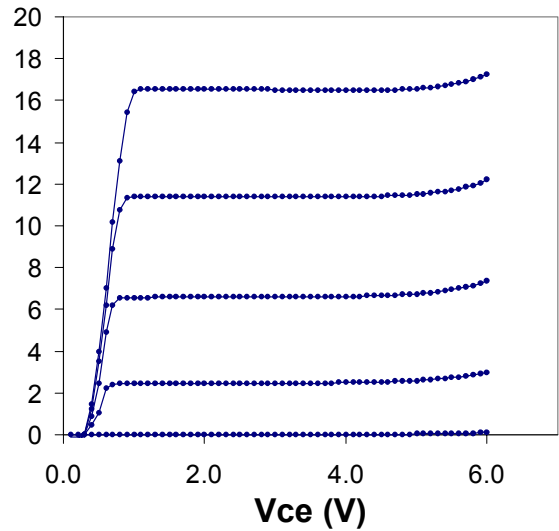


Fig. 5: Common-emitter I_c - V_{ce} characteristics of a $50 \times 50\ \mu\text{m}^2$ InAlAs/GaAsSb/InP DHBT with $4.5E19\ \text{cm}^{-3}$ base doping.

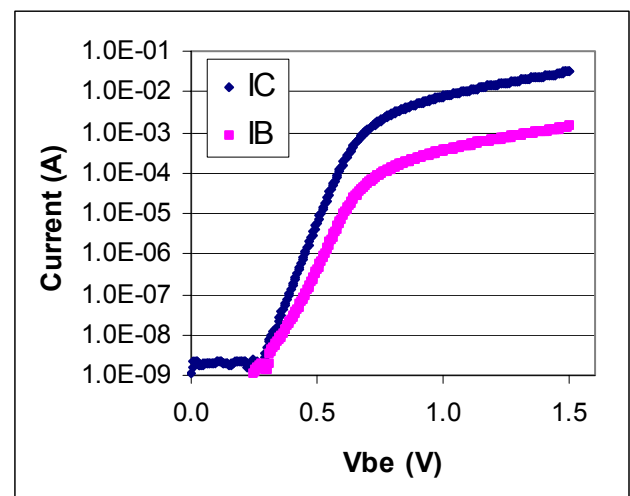


Fig. 6: Gummel plot of an InAlAs/GaAsSb/InP DHBT with base doping of $1E20\ \text{cm}^{-3}$.

IV. CONCLUSIONS

In summary, we have investigated GaAsSb DHBTs with

InP and InAlAs emitters using multi-wafer production MBE equipped with ABES and OFM sensors. State-of-the-art hole mobilities were obtained for 100 nm thick carbon-doped GaAsSb. We have also demonstrated that the Sb composition fluctuation is less than ± 0.1 % across a 4" wafer grown on a 4 X 4" platen. In contrast to InP emitters, GaAsSb based DHBTs with InAlAs emitters exhibited much better dc characteristics. The uniformity of GaAsSb and the excellent electrical properties of InAlAs/GaAsSb/InP DHBTs demonstrate that multi-wafer MBE is feasible for mass production of GaAsSb based DHBTs.

Acknowledgement

This work is partially supported by the DARPA TFAST program. The authors would like to thank Dr. Y. K. Chen and N. Weimann from Lucent Technologies for the DARPA-TFAST program management support, as well as DARPA-TFAST program manager Dr. J. C. Zolper for program support. Thanks also to A. Chen and J. Bettege for characterization and processing support.

References

- [1] W. Hafez, J. W. Lai, and M. Feng, *Electronics Letters*, vol. 39, pp.1475-1476, 2003.
- [2] DARPA-TFAST PI review, San Diego, Feb. 24-25, 2004.
- [3] C. R. Bolognesi, N. Matine, M. W. Dvorak, P. Yeo, X. G. Xu, and S. P. Watkins, *IEEE Trans. Electro Devices*, vol. 48, pp. 2631-2638, 2001.
- [4] N. Matine, M. W. Dvorak, S. Lam, C. R. Bolognesi, Y. M. Houg, and N. Moll, *Conf. Proc. of the 2000 Intl. Conf.*

on Indium Phosphide and Related Materials, pp. 239-242, 2003.

[5] C. R. Bolognesi, M. W. Dvorak, N. Matine, O. J. Pitts, and S. P. Watkins, *Jpn. J. Appl. Phys. Vol. 41*, pp. 1131-1135, 2002.

[6] M. W. Dvorak, C. R. Bolognesi, O. J. Pitts, and S. P. Watkins, *IEEE Electron Device Lett.*, vol 22, pp. 361-363, 2001.

[7] S. R. Johnson, C. Lavoie, T. Tiedje, and J. A. Mackenzie, *J. Vac. Sci. Technol. B*, vol. 11, pp. 1007-1110, 1993.

[8] J. A. Roth, T. J. De Lyon, and M. E. Adel, in *Proc. Mater. Res. Soc. Symp.*, vol. 324, pp. 353-356, 1994.

[9] P. Pinsukanjana, A. Jackson, J. Tofte, K. Maranowski, S. Campbell, J. English, S. Chalmers, L. Coldren, and A. Gossard, *JVST B*, vol.14 (3), pp. 2147-2150, 1996.

[10] P. R. Pinsukanjana, J. M. Marquis, J. Hubbard, M. A. Trivedi, R. F. Dickey, J. M.-S. Tsai, S. P. Kuo, P. S. Kao, and Y.C. Kao, *J. Crystal Growth*, vol. 251, pp. 124-127, 2003.

[11] M. J. Cherng, R. M. Cohen, and G. B. Stringfellow, *J. Electron Material*, vol. 13, pp. 799-813, 1984.

[12] S. P. Watkins, O. J. Pitts, C. Dale, X. G. Xu, M. W. Dvorak, N. Matine, and C. R. Bolognesi, *J. Crystal Growth*, vol. 221, pp. 59-65, 2000.

[13] S. S. Yi, S. J. Chung, H. Rohdin, M. Hueschen, D. Bour, N. Moll, D. R. Chamberlin, and J. Amano, *Conf. Proc. of the 2003 Intl. Conf. on Indium Phosphide and Related Materials*, pp.380-383, 2003.